

# Measurement of Electrical Potential of Repetitive Surface Dielectric Barrier Discharge in N<sub>2</sub> and O<sub>2</sub> Mixture Gas

T. Uemura<sup>1</sup>, A. Komuro<sup>2</sup> and R. Ono<sup>2</sup>

<sup>1</sup> Department of Electrical Engineering, The University of Tokyo

<sup>2</sup> Department of Advanced Energy, The University of Tokyo

**Abstract:** We measured the electrical potential and luminescence of surface dielectric barrier discharges in N<sub>2</sub> and O<sub>2</sub> mixture gas. The results show that the morphology of the discharge filaments depends on the polarity of AC voltage and oxygen concentration. Furthermore, the result shows that the charge distribution differs from the luminescence of the discharge. This indicates that the diffusion rates of the charges are different depending on the charge polarities.

**Keywords:** surface dielectric barrier discharge, Pockels effect

## 1. Introduction

Dielectric Barrier Discharge (DBD) has already been used in industrial applications such as surface treatment [1] and ozonizers [2], and recently there has been much research on air flow control using ionic wind generated by DBD [3]. DBD has a mechanism that cancels the external electric field by accumulating charge on the dielectric surfaces between the electrodes when an external electric field is applied, and by limiting the current, the discharge can be stable at atmospheric pressure. In particular, for surface dielectric barrier discharge (SDBD), a type of DBD, understanding the charge distribution on the dielectric surface is important to clarify its physical characteristics. The Pockels effect is used to measure surface potential [4]. The crystal used to measure the effect has the property that when a voltage  $V$  is applied, the light that passes through it has a phase difference  $\theta$  according to the potential as shown in Equation (1) due to its birefringence. Here,  $\lambda$  is the wavelength of the incident light,  $n_0$  is the refractive index of the crystal under normal conditions, and  $\gamma_{41}$  is the constant of the crystal.

$$\theta = \frac{2\pi}{\lambda} n_0^3 \gamma_{41} V \quad (1)$$

Bogaczyk *et al* [5] studied the DBD charge distribution of AC voltage in two symmetrical flat plates in helium and nitrogen, showing the difference in charge distribution during positive and negative polarity of AC voltage and the presence of residual charge after discharge. They also confirm the difference in the time response of the current depending on the type of gas. Mitsuhashi *et al* [6] measured the spatio-temporal distribution of potential on the dielectric surface during an AC voltage-induced SDBD and reported that the residual charge in the first cycle of AC voltage limits the progress of the discharge thereafter. Based on these previous studies, we investigated the change in the potential distribution on the dielectric surface in SDBD at AC voltages for different oxygen to nitrogen ratios. The discharge emission was also measured simultaneously with the potential distribution.

## 2. Experimental Setup

The optical system for measuring the surface potential and discharge emission of SDBD is shown in Fig 1,

consisting of an LED light source, polarizing beam splitter (PBS),  $\lambda/8$  wave plate, Pockels element, AC power supply and camera. In addition, the discharge area is covered by a reactor, which allows the gas to be replaced. The discharge electrode consists of a 1 mm thick BGO crystal as a dielectric material and a copper tape for the high-voltage electrode. The one side of the BGO crystal is coated by a transparent conducting (ITO) material for the ground electrode, and the other side is coated by dielectric mirror material to reflect the LED light.

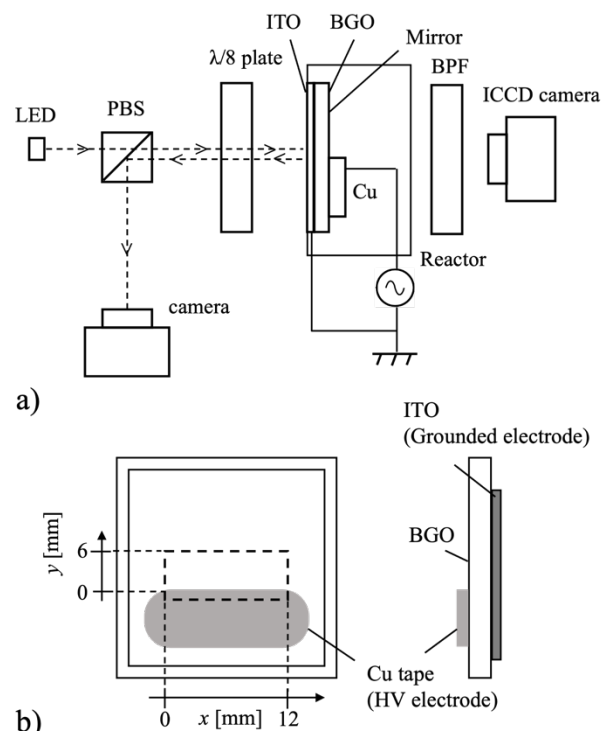


Fig 1. (a) Schematic view of the measurement system, and (b) Pockels crystal and electrode composition.

## 3. Results and Discussion

Fig 2 shows the potential distribution on the dielectric surface in N<sub>2</sub>, Air (N<sub>2</sub>:O<sub>2</sub> = 4:1), and O<sub>2</sub> at 10 kV<sub>PP</sub> and 1 kHz (cycle:  $T = 1$  ms) of AC voltage. Fig 2(a) and (b) at the positive and negative polarity peaks of the first cycle,

Fig 2(c) and (d) at the positive and negative polarity peaks of the second cycle, respectively. Fig 2(c) and (d) are the potential distributions at the positive and negative polarity peaks of the second cycle, respectively. In Fig 2(a), it can be seen that when positive voltage is applied, a thin and clear filament structure can be observed in  $N_2$ , while thick filaments with less branching structure can be seen in  $O_2$ . The potential distribution in Air seems to have a characteristic intermediate between those in  $O_2$  and  $N_2$ . In Fig 2(b), there is no filament distribution due to negative potential and the distribution is uniform in the  $x$  direction, but the spread in the  $y$  direction is largest in  $N_2$  and the spread of negative potential is smallest in  $O_2$ . In Fig 2(c) when positive voltage is applied in the second cycle, it can be seen that the filament's progress in the  $y$  direction is limited by the residual charge. This characteristic is particularly noticeable for discharges in Air and  $O_2$ , which can be attributed to the spread of the negative potential in the  $y$  direction in Fig 2(b).

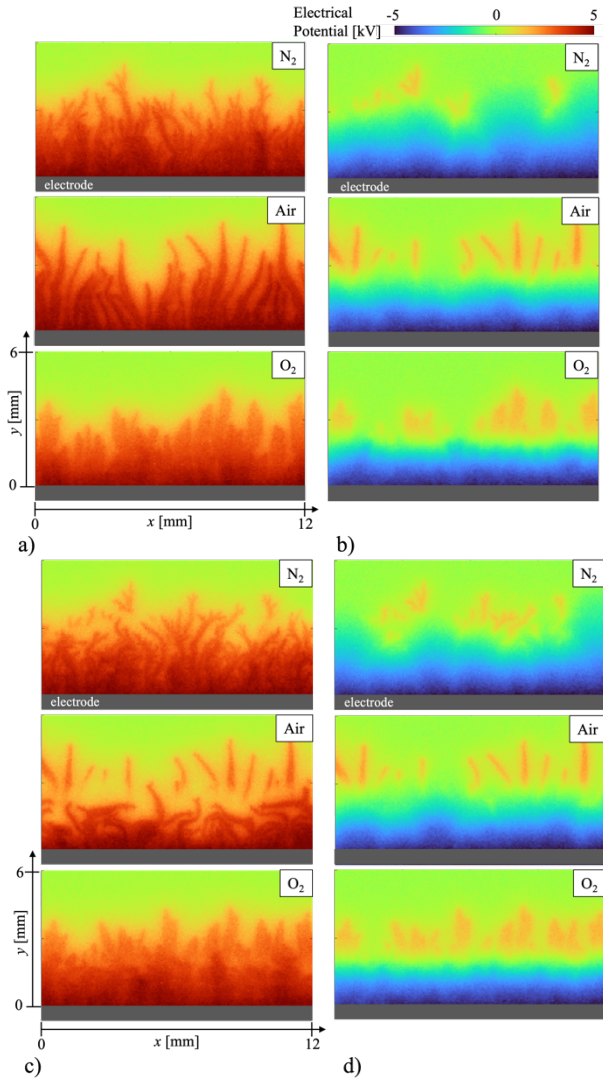


Fig 2. Spatial distribution of the electrical potential at (a)  $t = 1/4T$ , (b)  $3/4T$ , (c)  $5/4T$ , and (d)  $7/4T$  in  $N_2$ , Air and  $O_2$ .

Next, the potential distribution in the  $y$  direction averaged over the  $x$  direction from Fig 2 is shown in Fig 3. At  $t = 1/4T$ , the propagation of the positive potential distribution in the  $y$  direction is smaller for discharges in  $O_2$  than in  $N_2$ . Then, it is confirmed that positive charge remains from  $t = 2/4T$ , and at  $y \geq 2$  mm, the positive charge distribution remains close to that of  $t = 1/4T$ . Next, at  $t = 3/4T$ , in addition to the largest spread of negative polarity potentials in  $N_2$ , almost all of the remaining positive charge is removed in  $N_2$ . In  $O_2$ , on the other hand, the distribution of residual negative charge is also narrower than that of positive charge due to the fact that the spread of negative potential in the  $y$  direction is limited to residual positive charge at  $t = 3/4T$ .

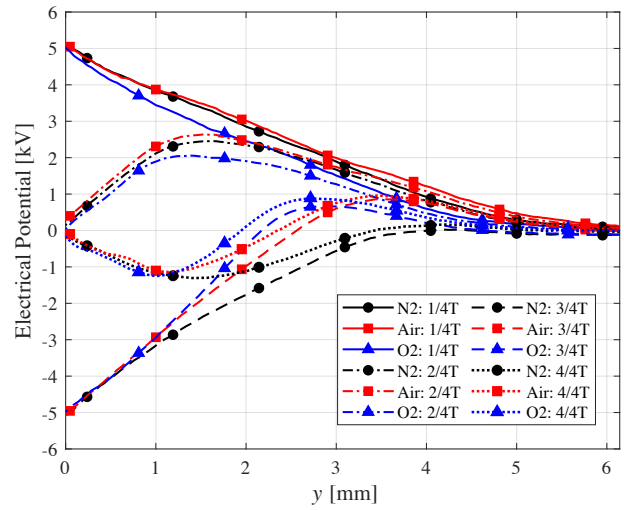


Fig 3. Electrical potential distribution in the  $y$  direction.

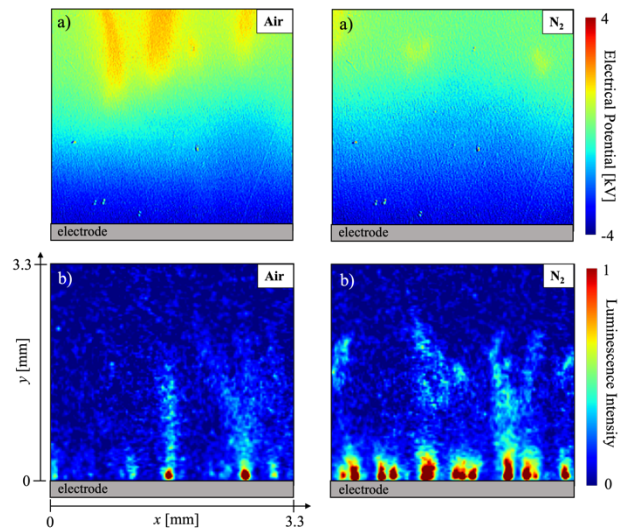


Fig 4. Comparison of (a) electrical potential and (b) discharge luminescence at  $2/4 < t/T < 3/4$ .

To investigate the relationship between discharge and potential distribution in negative polarity in detail, simultaneous measurement of potential distribution and discharge luminescence at  $2/4 < t/T < 3/4$  in the first negative polarity cycle is shown in Fig 4. The emission measurement shows a discharge filament of negative polarity, which was not visible in the potential distribution measurement by the Pockels effect. This result suggests that the charge distribution on the dielectric surface is different from the discharge distribution, which may be caused by the difference in the diffusion rates of the charges with different polarities, but further research is needed to clarify this phenomenon.

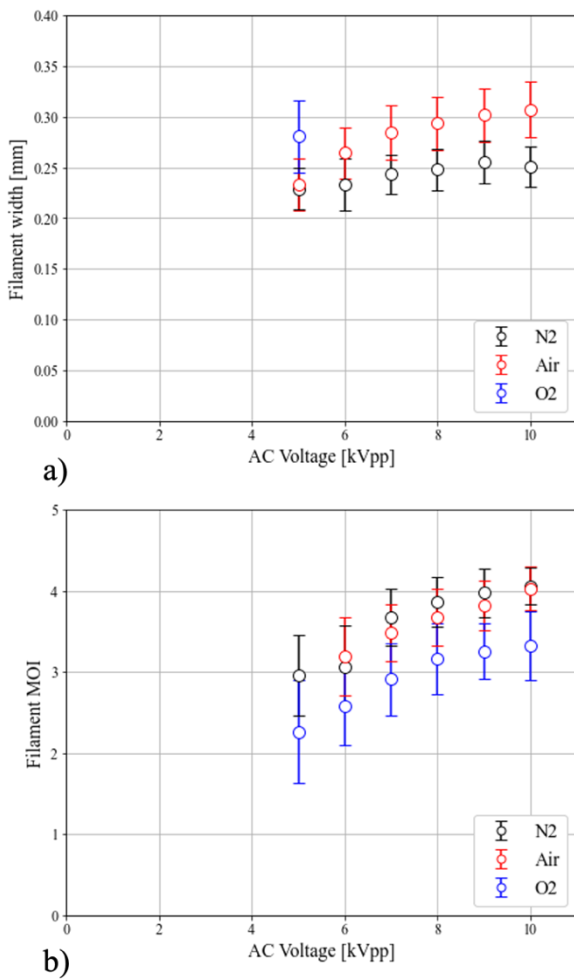


Fig 5. Relationships between applied voltage and (a) filament width and (b) filament MOI.

The dependence of filament width and Multiple Orientation Index (MOI) on AC voltage for positive polarity filaments after the second cycle are shown in Fig 5, which are obtained by image analysis [7]. Filaments in O<sub>2</sub> are analyzed only at 5 kV<sub>PP</sub> in Fig 5(a) because it is difficult to distinguish each filament as a single filament due

to their overlap. From Fig 5(a), it is confirmed that the filament in N<sub>2</sub> is the thinnest. It can also be seen that the filaments become thicker as the applied voltage increases. In Fig 5(b), MOI is defined by equation (2), where  $p(\theta)$  is the probability of occurrence for the filament direction  $\theta$  obtained from image analysis. In other words, the smaller MOI, the greater the directional bias of the filament structure.

$$MOI = - \sum p(\theta) \log_2 p(\theta) \quad (2)$$

Then, MOI is the smallest in O<sub>2</sub>, which suggests that the filaments have less bending. We also believe that the amount of filament bending and branching structure in N<sub>2</sub> and Air changes which MOI is greater at each voltage value.

#### 4. Conclusion

The potential distribution of SDBD in a mixture of N<sub>2</sub> and O<sub>2</sub> gases was measured by the Pockels effect. As a result, differences in the potential distribution depending on the polarity of the voltage and the residual charge were observed. The filament at the first cycle of positive voltage was different in N<sub>2</sub>, with a thin, branchy structure; in Air, a clear structure with no branching; and in O<sub>2</sub>, a thick, indistinct structure. In addition, it was found that while the progress of the discharge is hindered by the residual positive charge in the second cycle of AC voltage in O<sub>2</sub>, the progress of the discharge is not significantly hindered after the second cycle in N<sub>2</sub> due to the remarkable spread of negative potentials. Furthermore, measurement of discharge luminescence at negative polarity revealed filaments that were not observed in the charge distribution, suggesting that the discharge distribution differs from the charge distribution. Finally, we measured the thickness of the filaments at positive polarity after the second cycle and confirmed that the filaments were thinnest in N<sub>2</sub>. The analysis of the filament direction suggested that there is less presence of bending in the filaments in O<sub>2</sub>, and that the branching increases with increasing percentage of N<sub>2</sub>.

#### 5. References

- [1] Morent R, De Geyter N, Gengembre L, Leys C, Payen E, Van Vlierberghe S and Schacht E, *EPJ Applied Physics*, **43**, 289-294 (2008)
- [2] Jodzis S and Zięba M, *Vacuum*, **155**, 29-37 (2018)
- [3] Wang J J, Choi K S, Feng L H, Jukes T N and Whalley R D, *Prog. Aerosp. Sci.*, **62**, 52-78 (2013)
- [4] Tanaka D, Matsuoka S, Kumada A and Hidaka K, *J. Phys. D: Appl. Phys.*, **42**, 075204 (2009)
- [5] Bogaczyk M, Wild R, Stollenwerk L and Wagner H E, *J. Phys. D: Appl. Phys.*, **45**, 465202 (2012)
- [6] Mitsuhashi K, Komuro A, Suzuki K, Natsume C and Ando A, *Plasma Sources Sci. Technol.*, **30**, 04LT02 (2021)
- [7] Kimori Y, Hikino K, Nishimura M and Mano S, *J. Theor. Biol.*, **389**, 123-131 (2016)